

The origin of dust in galaxies revisited: the mechanism determining dust content

Akio K. Inoue¹¹College of General Education, Osaka Sangyo University, 3-1-1 Nakagaito, Daito, Osaka 574-8530

(Received xxxx xx, 2010; Revised xxxx xx, 2010; Accepted xxxx xx, 2010; Online published Xxxxxx xx, 2008)

The origin of cosmic dust is a fundamental issue in planetary science. This paper revisits the origin of dust in galaxies, in particular, in the Milky Way, by using a chemical evolution model of a galaxy composed of stars, interstellar medium, metals (elements heavier than helium), and dust. We start from a review of time-evolutionary equations of the four components, and then, we present simple recipes for the stellar remnant mass and yields of metal and dust based on models of stellar nucleosynthesis and dust formation. After calibrating some model parameters with the data from the solar neighbourhood, we have confirmed a shortage of the stellar dust production rate relative to the dust destruction rate by supernovae if the destruction efficiency suggested by theoretical works is correct. If the dust mass growth by material accretion in molecular clouds is active, the observed dust amount in the solar neighbourhood is reproduced. We present a clear analytic explanation of the mechanism for determining dust content in galaxies after the activation of accretion growth: a balance between accretion growth and supernova destruction. Thus, the dust content is independent of the uncertainty of the stellar dust yield after the growth activation. The timing of the activation is determined by a critical metal mass fraction which depends on the growth and destruction efficiencies. The solar system formation seems to have occurred well after the activation and plenty of dust would have existed in the proto-solar nebula.

Key words: Cosmic dust — physical processes of dust in the interstellar medium — galaxy evolution

1. Introduction

Cosmic dust grains are negligible in mass in the Universe. Nevertheless, they play significant roles on a lot of astronomical, astrophysical, and astrochemical aspects: extinction (absorption and scattering) of radiation, an emission source in infrared wavelengths, a coolant and a heat source in the interstellar medium (ISM) and intergalactic medium (IGM), and a site of formation of molecules. Therefore, dust is one of the most important ingredients in the Universe. Dust is also important for planetary science because grains are material for planets.

Dust grains are formed in rapidly cooling gas of stellar outflows (Yamamoto & Hasegawa 1977; Draine & Salpeter 1977). We call such grains ‘stardust’. Sources of the stardust are asymptotic giant branch (AGB) stars, supernovae (SNe), red supergiants, novae, Wolf-Rayet stars, and so on (e.g., Gehr 1989). The main source of the stardust in the present Milky Way and the Magellanic Clouds is thought to be AGB stars (Gehrz 1989; Draine 2009; Matsuura et al. 2009).

SNe may also produce a significant amount of stardust (Kozasa & Hasegawa 1987; Todini & Ferrara 2001; Nozawa et al. 2003, 2007; Schneider et al. 2004; see also Kozasa et al. 2009). Stardust from SNe is particularly important in the early Universe because the time for stars to evolve to the AGB phase is typically about 1 Gyr, but the cosmic time in the early Universe is shorter than it (Morgan & Edmunds 2003; Maiolino et al. 2004; Dwek et al. 2007; but see also Valiante et al. 2009). The ‘first’ stardust may also play an

important role to change the mode of star formation from massive star dominated to present-day Sun-like star dominated (Schneider et al. 2003, 2006).

However, dust formation by SNe remains in controversy observationally. First detections of a few M_{\odot} dust freshly formed, which is much larger than expected, in Cassiopeia A (Cas A) and Kepler SN remnants (SNRs) by submillimeter observations with *SCUBA* (Dunne et al. 2003; Morgan et al. 2003) were almost contaminated by foreground dust in the ISM on the sight-lines (Krouze et al. 2004; Gomez et al. 2009). Recent infrared observations with *Spitzer Space Telescope* and *AKARI* and submillimeter observations with *Herschel* and *BLAST* of Cas A and other SNRs are agreeing with theoretical expectations of 0.01–0.1 M_{\odot} per one SN (Rho et al. 2008; Sakon et al. 2009; Nozawa et al. 2010; Barlow et al. 2010; Sibthorpe et al. 2010).

Once stardust grains are injected into the ISM, they are processed there. The grains in hot gas are bombarded by thermally moving protons and sputtered (Onaka & Kamijo 1978; Draine & Salpeter 1979). SN shock waves probably destroy dust grains by grain–grain collisional shattering as well as sputtering (e.g., Dwek & Arendt 1992; Jones et al. 1994, 1996; Nozawa et al. 2006; Silvia et al. 2010). This destruction process is widely accepted and observational evidences of the destruction have been found in several SNRs, especially with *Spitzer Space Telescope* (Arendt et al. 1991, 2010; Borkowski et al. 2006; Williams et al. 2006; Dwek et al. 2008; Sankrit et al. 2010; but see Mouri & Taniguchi 2000).

Assuming the destruction efficiency expected by theoretical works, we obtain the life-time of dust grains of the order of 100 Myr (McKee 1989; Draine 1990; Jones et al. 1994,

Copy right© The Society of Geomagnetism and Earth, Planetary and Space Sciences (SGEPSS); The Seismological Society of Japan; The Volcanological Society of Japan; The Geodetic Society of Japan; The Japanese Society for Planetary Sciences; TERRAPUB.

1996). On the other hand, the injection time of stardust is of the order of 1 Gyr (e.g., Gehrz 1989). Thus, another efficient channel of dust formation is required to keep dust content in galaxies. The most plausible mechanism is the accretion growth in the ISM (Draine 1990, 2009); in dense molecular clouds, atoms and molecules of some refractory elements and compounds accrete onto pre-existent grains and may change from the gas phase to the solid phase. Note that unlike the sticking growth of grains well studied in protoplanetary disks, this accretion growth causes an increase in dust mass. This type of growth is favored to explain the observed depletions of some elements in the gas phase of the ISM relative to the solar abundance. The correlation between the depletion degree and the density in the ISM is particularly suggestive for this process (e.g., Savage & Sembach 1996; Jenkins 2009). It is also suggested that an efficient growth is required to explain massive dust mass observed in the early Universe (Michałowski et al. 2010).

Since the pioneering work by Dwek & Scalo (1980), many theoretical works on dust content evolution in galaxies have been made so far (Dwek 1998; Lisenfeld & Ferrara 1998; Edmunds & Eales 1998; Hirashita 1999a,b,c; Edmunds 2001; Hirashita et al. 2002; Inoue 2003; Morgan & Edmunds 2003; Dwek et al. 2007; Zhukovska et al. 2008; Calura et al. 2008; Valiante et al. 2009; Pipino et al. 2011; Dwek & Cherchneff 2011; Gall et al. 2011a,b; Mattsson 2011; Asano et al. 2011). These works are based on the evolutionary model of elemental abundance in galaxies called chemical evolution model (Tinsley 1980 for a review) and add some (or all) of the three processes of formation, destruction, and growth of dust to it. One of the main results from the recent works is the importance of the accretion growth.

This paper presents a new interpretation of the mechanism for determining dust content in galaxies. Previous works imply that the mechanism is a balance between dust destruction by SNe and accretion growth in the ISM. However, this point has not been discussed clearly, in contrast, this paper analytically shows that it is. For this aim, a simple one-zone model is sufficient. In addition, we present new simple recipes describing stellar remnant mass and yields of elements and dust from state-of-the-art models of stellar nucleosynthesis and formation of stardust.

We will start from a review of basic equations presented in §2. In §3, we present new simple recipes of stellar remnant mass and yields. In §4, we calibrate some model parameters to reproduce the observed properties of the solar neighborhood. In §5, we present our analytical interpretation of the mechanism for determining dust content in galaxies. We will present some further discussions in §6. Experts of this field may go straight to §5 which is the new result of this paper.

Throughout this paper, we call elements heavier than helium ‘metal’ according to the custom of astronomy. We adopt the metal mass fraction (so-called metallicity) in the Sun of $Z_{\odot} = 0.02$ (Anders & Grevesse 1989) conventionally, although the recent measurements suggest a smaller value of 0.0134 (Asplund et al. 2009).

2. Chemical and dust evolution model of galaxies

2.1 Equations of chemical and dust amount evolution

We deal with a galaxy composed of stars (including their remnants; i.e. white dwarfs, neutron stars, and black-holes) and the ISM. For simplicity, we assume the ISM to be one-zone. The ISM contains metal and dust as internal components. If we denote masses of these components as M_* (stars [and remnants]), M_{ISM} (ISM), M_Z (metal), and M_d (dust), the equations describing their time evolutions are (e.g., Dwek 1998)

$$\frac{dM_*}{dt} = S(t) - R(t), \quad (1)$$

$$\frac{dM_{\text{ISM}}}{dt} = -S(t) + R(t) + I(t) - O(t), \quad (2)$$

$$\frac{dM_Z}{dt} = -Z(t)S(t) + Y_Z(t) + I_Z(t) - O_Z(t), \quad (3)$$

$$\frac{dM_d}{dt} = -Z_d(t)S(t) + Y_d(t) - D_{\text{SN}}(t) + G_{\text{ac}}(t) + I_d(t) - O_d(t), \quad (4)$$

where S is the star formation rate, R is the mass return rate from dying stars, Y_Z and Y_d are the metal and dust supplying rates ‘yields’ by dying stars, respectively. $Z \equiv M_Z/M_{\text{ISM}}$ is the metal mass fraction in the ISM called ‘metallicity’, and $Z_d \equiv M_d/M_{\text{ISM}}$ is the dust mass fraction in the ISM which we call the dust-to-gas mass ratio. Note that $M_{\text{ISM}} > M_Z \geq M_d$.

I , I_Z , and I_d are the ISM, metal, and dust infall rates from the IGM, respectively. O , O_Z , and O_d are the ISM, metal, and dust outflow rates to the IGM, respectively. In this paper, we do not consider any outflows ($O = O_Z = O_d = 0$), but consider only an ISM infall I (no metal and dust in infalling gas: $I_Z = I_d = 0$), which is required to reproduce the metallicity distribution of stars nearby the Sun.¹ The reason why we omit any outflows is that we do not know the transport mechanism of metal and dust from galaxies to the IGM (e.g., Bianchi & Ferrara 2005). However, this omission may be inconsistent with detections of metal and dust in the IGM (e.g., Songaila & Cowie 1996; Ménard et al. 2010).²

In the dust mass equation (eq. [4]), there are two additional terms; D_{SN} is the dust destruction rate by SNe and G_{ac} is the dust growth rate in the ISM by metal accretion. These two terms are discussed in §2.5 and §2.6 in detail.

2.2 Star formation and infall rates

We adopt a simple recipe for star formation introduced by Schmidt (1959): $S \propto M_{\text{ISM}}^p$ (Schmidt law). The index p called Schmidt index is observationally indicated to be

¹Without gas infall from the intergalactic space, we expect a much larger number of low-metallicity stars at the solar neighborhood than the observed. This is called the ‘G-dwarf problem’ (e.g., Pagel 1989).

²The origin of intergalactic metals and dust is galactic outflows and the amount ejected from galaxies is the same order of that remained in galaxies (e.g., Ménard et al. 2010 for dust; see also Inoue & Kamaya 2003, 2004, and 2010). Dust grains may be ejected from galaxies more efficiently than metals because the grains receive momentum through radiation pressure (Bianchi & Ferrara 2005). Even in this case, our discussion about the dust-to-metal ratio in §5 would not be affected essentially by omission of this selective removal of dust, although the set of model parameters which can reproduce the observations would change. In any case, this point would be an interesting future work.

$p = 1-2$ (e.g., Kennicutt 1998; Elmegreen 2011) and some theoretical interpretations for the value are presented (e.g., Dopita & Ryder 1994). However, the value and its origin of the index is still an open problem (Elmegreen 2011 and references therein). Fortunately, the choice of the index is not important in fact because in §4 we calibrate other model parameters so as to reproduce the observed star formation history $S(t)$ at the solar neighborhood which is essential. We here assume $p = 1$ in order to solve the equations analytically in §5. In this case, we need a time-scale to give the star formation rate: star formation time-scale, τ_{SF} (see Table 1 in §4 for the values). Thus, the star formation rate is given by

$$S(t) = \frac{M_{\text{ISM}}(t)}{\tau_{\text{SF}}}. \quad (5)$$

The infall from the IGM mimics the structure formation in the Universe based on the hierarchical scenario with cold dark matter (e.g., Peacock 1999); small galaxies are first formed at density peaks of the dark matter distribution in the Universe and they grow up larger and larger as they merge each other and also obtain mass by accretion process. Here we simply assume a smooth exponential infall rate although the mass assembly of a galaxy is intrinsically episodic due to the merging process. This simplification is a kind of ensemble average of many galaxies and appropriate to examine a mean property of the galaxies. The infall rate which we adopt is

$$I(t) = \frac{M_{\text{total}}}{\tau_{\text{in}}} \exp(-t/\tau_{\text{in}}), \quad (6)$$

where τ_{in} is the infall time-scale and M_{total} is the total mass which a galaxy obtains within the infinite time (see Table 1 in §4 for the values). Note that M_{total} just gives the normalization of mass of a galaxy.

2.3 Stellar mass spectrum and returned mass rate

Salpeter (1955) first investigated the mass spectrum of stars in the solar neighborhood, corrected it for the modulation by stellar evolution and death, and obtained the mass spectrum of stars when they are born, called initial mass function (IMF) of stars. The Salpeter's IMF is a power-law: $dN/dm = \phi(m) \propto m^{-q}$ with $q = 2.35$. A lot of following researches confirmed that the slope was quite universal, especially for massive stars, although there was a cut-off mass for low mass stars (e.g., Kroupa 2002, Chabrier 2003 for reviews). We adopt here a simple functional from proposed by Larson (1998) which is essentially equivalent to the IMFs by Kroupa (2002) and Chabrier (2003) as

$$\phi(m) \propto m^{-q} \exp(-m_c/m), \quad (7)$$

with a cut-off mass m_c and the range from m_{low} to m_{up} . As a standard case, we adopt $p = 2.35$, $m_c = 0.2 M_{\odot}$, $m_{\text{low}} = 0.1 M_{\odot}$, and $m_{\text{up}} = 100 M_{\odot}$. The cut-off mass well matches with the observed data compiled by Kroupa (2002). We normalize the IMF as $\int_{m_{\text{low}}}^{m_{\text{up}}} m \phi(m) dm = 1$.

The mass returned rate from dying stars, R , is given by

$$R(t) = \int_{m_{\text{lf}}(t)}^{m_{\text{up}}} \{m - w(m, Z[t'])\} \phi(m) S(t') dm, \quad (8)$$

where

$$t' = t - \tau_{\text{lf}}(m) \quad (9)$$

is the time at which stars with mass m dying at time t are born, $\tau_{\text{lf}}(m)$ is the stellar life-time, $w(m, Z)$ is the remnant mass of stars with mass m and metallicity Z , and $m_{\text{lf}}(t)$ is the minimum mass of stars dying at time t . This is the inverse function of $t = \tau_{\text{lf}}(m)$. If time t is less than the life-time of the star with m_{up} , the returned rate $R = 0$. We have assumed that the metallicity of a star is the same as the ISM metallicity at the time when the star is born.

The stellar life-time $\tau_{\text{lf}}(m)$ is calculated by the formula of Raiteri et al. (1996) which is a fitting function of Padova stellar evolutionary tracks (Bertelli et al. 1994). This formula is a function of stellar mass m and metallicity Z . However, the Z -dependence is weak. Thus, we neglect it (we always set $Z = Z_{\odot}$ in the formula).

2.4 Stellar yields of 'metal' and dust

When stars die, they eject substantial mass of metal and dust into the ISM. The term driving the time evolution of metal mass given by equation (3) is the metal supplying rate, Y_Z , called metal yield. Using the IMF, $\phi(m)$, and the star formation rate, $S(t)$, we can express the metal yield as

$$Y_Z(t) = \int_{m_{\text{lf}}(t)}^{m_{\text{up}}} m_Z(m, Z[t']) \phi(m) S(t') dm, \quad (10)$$

where m_Z is the metal mass ejected from a star with mass m and metallicity Z , and t' is given by equation (9).

The dust supplying rate, Y_d , called dust yield can be expressed likewise:

$$Y_d(t) = \int_{m_{\text{lf}}(t)}^{m_{\text{up}}} m_d(m, Z[t']) \phi(m) S(t') dm, \quad (11)$$

where m_d is the dust mass ejected from a star with mass m and metallicity Z , and t' is given by equation (9).

2.5 Dust destruction by supernova blast waves

Dust grains are destroyed by SN shock waves due to shattering and sputtering (e.g., Dwek & Arendt 1992). This dust destruction are observed in some SNRs as described in §1. In this paper, we adopt the dust destruction rate by SNe proposed by Dwek & Scalo (1980) and McKee (1989):

$$D_{\text{SN}}(t) = \frac{M_d(t)}{\tau_{\text{SN}}(t)}, \quad (12)$$

where the destruction time-scale τ_{SN} is defined as the time-scale which all the ISM is swept by 'dust destructive' shock waves:

$$\tau_{\text{SN}}(t) = \frac{M_{\text{ISM}}(t)}{\epsilon m_{\text{SN}} R_{\text{SN}}(t)}, \quad (13)$$

where R_{SN} is the SN occurrence rate, m_{SN} is the mass swept by a single SN, and ϵ is the efficiency of the dust destruction. The SN occurrence rate is given by

$$R_{\text{SN}}(t) = \int_{8M_{\odot}}^{40M_{\odot}} \phi(m) S(t') dm, \quad (14)$$

where we have assumed the mass range for SNe to be 8–40 M_{\odot} (Heeger et al. 2003) and t' is in equation (9). If $t < \tau_{\text{lf}}(40 M_{\odot})$, $R_{\text{SN}} = 0$. Note that we consider only Type II SNe and neglect Type Ia SNe. The reason is discussed in §3.

The effective mass swept by dust destructive shock wave, ϵm_{SN} is the important parameter. It is estimated to be $\sim 1000 M_{\odot}$, namely $\epsilon \sim 0.1$ and $m_{\text{SN}} \sim 10^4 M_{\odot}$ (McKee 1989, Nozawa et al. 2006). Recent models for starburst galaxies in the early Universe often assume an effective mass of $\epsilon m_{\text{SN}} \sim 100 M_{\odot}$ which is a factor of 10 smaller than our fiducial value (Dwek et al. 2007; Pipino et al. 2011; Gall et al. 2011a). Their argument is that starburst activity produces multiple SNe which make the ISM highly inhomogeneous and the dust destruction efficiency decreases in such medium. However, the solar neighborhood is not the case, and thus, we keep $\epsilon m_{\text{SN}} \sim 1000 M_{\odot}$.

2.6 Dust growth by ‘metal’ accretion in the ISM

In the ISM, atoms of some refractory elements (or refractory molecules) may accrete onto a dust grain and may become a part of the grain. We call this process the accretion growth of dust in the ISM (Draine 1990). Note that this process does not need nucleation, and thus, can occur even in the ISM. A simple estimate of the growth rate is (e.g., Hirashita 2000)

$$G_{\text{ac}}(t) = X_{\text{cold}} N_{\text{d}}(t) \pi a^2 s_Z v_Z \rho_Z^{\text{gas}}(t), \quad (15)$$

where $X_{\text{cold}} N_{\text{d}}$ is the number of dust grains in cold dense clouds, a is the grain radius, s_Z is the sticking probability of accreting metals (atoms or molecules), v_Z is the thermal velocity of the accreting metals and ρ_Z^{gas} is the mass density of the accreting metals in the gas-phase. Note that all the quantities except for $X_{\text{cold}} N_{\text{d}}$ in equation (15) are typical (or effective) values averaged over various grain radii, elements, and ISM phases. The gas-phase metal density is reduced to $\rho_Z^{\text{gas}} = \rho_{\text{ISM}}^{\text{eff}} Z(1 - \delta)$, where $\rho_{\text{ISM}}^{\text{eff}}$ is an effective ISM mass density. We define it as a mass-weighted average density of various ISM phases, and then, it is determined by the density of dense molecular clouds where the dust growth occurs. Note that $\delta = M_{\text{d}}/M_Z$, the dust-to-metal mass ratio (the dust depletion factor is $1 - \delta$). For spherical grains, $N_{\text{d}} = 3M_{\text{d}}/(4\pi a^3 \sigma)$, where σ is the typical material density of grains.

Equation (15) can be reduced to

$$G_{\text{ac}}(t) = \frac{M_{\text{d}}(t)}{\tau_{\text{ac}}(t)}. \quad (16)$$

The accretion growth time-scale τ_{ac} is

$$\tau_{\text{ac}}(t) = \frac{\tau_{\text{ac},0}}{Z(t)(1 - \delta[t])}, \quad (17)$$

where the normalization $\tau_{\text{ac},0}$ is the parameter determining the process:

$$\tau_{\text{ac},0} = \frac{4a\sigma}{3X_{\text{cold}} s_Z v_Z \rho_{\text{ISM}}^{\text{eff}}}. \quad (18)$$

This time-scale is very uncertain, but we will obtain $\tau_{\text{ac},0} = 3 \times 10^6$ yr as the fiducial value in §4.2 in order to reproduce the dust-to-metal ratio at the solar neighborhood with the SN destruction efficiency of $\epsilon m_{\text{SN}} = 1000 M_{\odot}$. This value can be obtained with a set of parameters of $a = 0.1 \mu\text{m}$ (typical size in the ISM of the Milky Way), $\sigma = 3 \text{ g cm}^{-3}$ (compact silicates), $s_Z = 1$, $v_Z = 0.2 \text{ km s}^{-1}$

(^{56}Fe as an accreting metal atom and thermal temperature of 100 K), $\rho_{\text{ISM}}^{\text{eff}} = 1 \times 10^{-22} \text{ g cm}^{-3}$, and $X_{\text{cold}} = 0.2$. This set is just an example but ensures that the time-scale is not outrageous.

There is a discussion about the lifetime of dense clouds (or recycling time-scale of dense gas) should be longer than the accretion growth time-scale for an efficient dust growth (Zhukovska et al. 2008; Dwek & Cherchneff 2011). According to these authors, the lifetime is long enough to realize an efficient dust growth in the Milky Way and even in starburst in the early Universe. Another issue is the effect of grain size distribution which is discussed in Hirashita (2011).

3. Stellar remnant and ‘metal’ and dust yields

In this section, we present new simple formulas to describe the stellar remnant mass and yields of metal and dust which are useful to input into chemical evolution codes. We represent all elements heavier than helium as just a ‘metal’ in the formulas for simplicity, while yields of various elements are presented in literature. We consider three types of stellar death: white dwarfs through the AGB phase, core-collapse Type II SNe, and direct collapse toward black-hole called ‘collapser’ (Heger et al. 2003). In this paper, we assume the mass range for the SNe to be 8–40 M_{\odot} (Heger et al. 2003). The stars with mass below or above this mass range become AGB stars or ‘collapsers’, respectively.

We neglect Type Ia SNe for simplicity. This population of SNe is the major source of iron element (Iwamoto et al. 1999) and may be the source of iron dust (Calura et al. 2008). However, in respect of the total stardust mass budget, the contribution relative to SNe II is always less than 1–10% (Zhukovska et al. 2008; Pipino et al. 2011). Since we are dealing with metal and dust as each a single component, we safely neglect the contribution of SNe Ia.

The remnant mass, $w(m, Z)$, is taken from model calculations of AGB stars (Karakas 2010) and SNe (Nomoto et al. 2006). Figure 1 shows the remnant mass fraction relative to the initial stellar mass, w/m . This depends on metallicity Z because Z in the stellar atmosphere determines radiation pressure through opacity and the strength of the stellar wind in the course of the stellar evolution, and affects the remnant mass. However, as shown in Figure 1, the dependence is weak, so we neglect it. We obtain the following fitting formula:

$$\frac{w(m)}{m} = \begin{cases} 1 & (m > 40 M_{\odot}) \\ 0.13 \left(\frac{m}{8 M_{\odot}} \right)^{-0.5} & (8 M_{\odot} \leq m \leq 40 M_{\odot}) \\ 0.13 \left(\frac{m}{8 M_{\odot}} \right)^{-0.7} & (m < 8 M_{\odot}) \end{cases}, \quad (19)$$

which is shown by the solid line in Figure 1. This fitting formula agrees with the values in Table 1 of Morgan & Edmunds (2003) within a $< 20\%$ difference, except for $m = 9 M_{\odot}$ case in which our estimate is a factor of 2 lower than that of Morgan & Edmunds (2003).

For the metal yield, m_Z , we adopt the data taken from model calculations of AGBs (Karakas 2010) and SNe (Nomoto et al. 2006). Figure 2 shows m_Z relative to the initial stellar mass m as a function of m . While the expected m_Z depends on mass m and metallicity Z by a complex way,

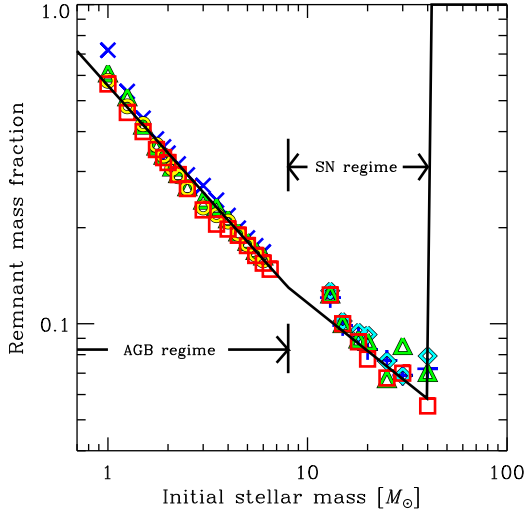


Fig. 1. Remnant mass fraction, w/m , as a function of the initial stellar mass, m . The data of AGB stars ($1-8 M_{\odot}$) are taken from Karakas (2010) and those of SNe ($8-40 M_{\odot}$) are taken from Nomoto et al. (2006). The different symbols indicate different metallicity Z : $Z = 0$ (plus), $Z = 0.0001$ (cross), $Z = 0.001$ (diamond), $Z = 0.004$ (triangle), $Z = 0.008$ (circle), and $Z = 0.02$ (square). The solid line is a fitting function given by equation (19).

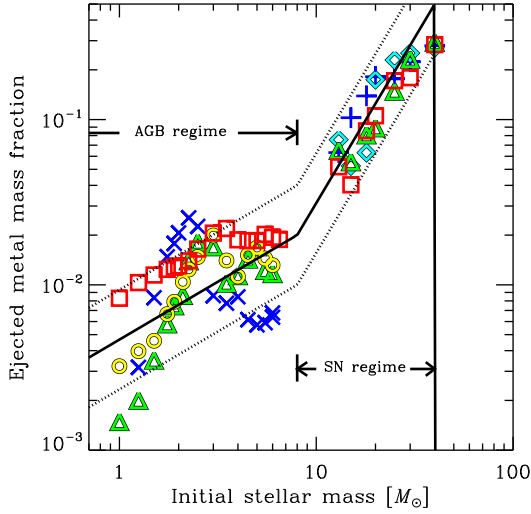


Fig. 2. Ejected metal mass fraction, m_Z/m , as a function of the initial stellar mass, m . The data of AGB stars ($1-8 M_{\odot}$) are taken from Karakas (2010) and those of SNe ($8-40 M_{\odot}$) are taken from Nomoto et al. (2006). The meaning of the symbols are the same as in Fig. 1. The solid line is a fitting function given by equation (20). The dotted lines are the cases a factor of two higher or lower than the solid line.

we approximate the data with a simple power-law of only m as

$$\frac{m_Z(m)}{m} = \begin{cases} 0 & (m > 40 M_{\odot}) \\ f_Z \left(\frac{m}{8 M_{\odot}} \right)^2 & (8 M_{\odot} \leq m \leq 40 M_{\odot}) \\ f_Z \left(\frac{m}{8 M_{\odot}} \right)^{0.7} & (m < 8 M_{\odot}) \end{cases} \quad (20)$$

When the normalization $f_Z = 0.02$, equation (20) is the solid line in Figure 2. As shown in the figure, the uncertainty of equation (20) is a factor of ~ 2 . This fitting agrees with

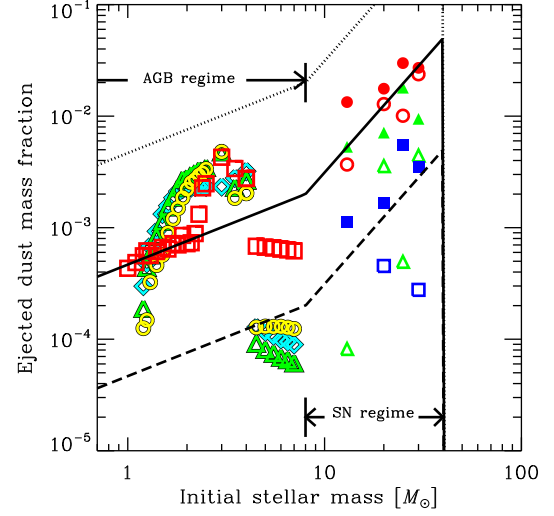


Fig. 3. Ejected dust mass fraction, m_d/m , as a function of the initial stellar mass, m . The data of AGB stars ($1-8 M_{\odot}$) are taken from Zhukovska et al. (2008) and those of SNe ($8-40 M_{\odot}$) are taken from Nozawa et al. (2007). For the AGB data, the different symbols indicate different metallicity Z : $Z = 0.001$ (diamond), $Z = 0.004$ (triangle), $Z = 0.008$ (circle), and $Z = 0.02$ (square). For the SNe data, the different symbols indicate different ambient hydrogen density $n_H = 0.1 \text{ cm}^{-3}$ (circle), $n_H = 1 \text{ cm}^{-3}$ (triangle), and $n_H = 10 \text{ cm}^{-3}$ (square). The open and filled symbols correspond to ‘mixed’ or ‘unmixed’ cases of Nozawa et al. (2007), respectively. The dotted, solid, and dashed lines are the cases of $\xi = 1, 0.1$, and 0.001 , respectively, in equation (21).

the values in Table 1 of Morgan & Edmunds (2003) within a factor of 2 difference in the SN regime. However, in the AGB regime, the difference is as large as the model results by Karakas (2010). The effect of this large uncertainty of the yield is discussed in §6.1.

The dust yield, m_d , calculated by Zhukovska et al. (2008) and Ferrarotti & Gail (2006) for AGBs and Nozawa et al. (2007) for SNe are shown in Figure 3. These yields are theoretical ones and do not seem to be compared with observations very much yet. As found in Figure 3, m_d depends on mass m and metallicity Z by a complex way as the metal yield m_Z does. Moreover, the dust production by SNe is further complex because the reverse shock moving in the ejecta of a SN may destroy the dust produced in the ejecta (Bianchi & Schneider 2007, Nozawa et al. 2007, Nath et al. 2008, Silvia et al. 2010). This self-destruction depends on the material strength against the destruction³ and the ambient gas density which determines the strength of the reverse shock. According to Nozawa et al. (2007), we plot three cases of the ambient density and ‘mixed’ and ‘unmixed’ dust productions⁴ in Figure 3. We adopt a simple formula for m_d as

$$m_d(m) = \xi m_Z(m), \quad (21)$$

where ξ is a scaling factor and means an efficiency of con-

³The micro-process of the destruction considered in Nozawa et al. (2007) is sputtering by hot gas.

⁴The ‘mixed’ and ‘unmixed’ mean the elemental mixing in the SN ejecta (Nozawa et al. 2003). In the ‘mixed’ case, there is no layer where C is more abundant than O, then, only silicate, troilite, and corundum grains can be formed. On the other hand, the ‘unmixed’ case has a C-rich layer and Fe layer and can form carbon and iron grains as well as silicate.

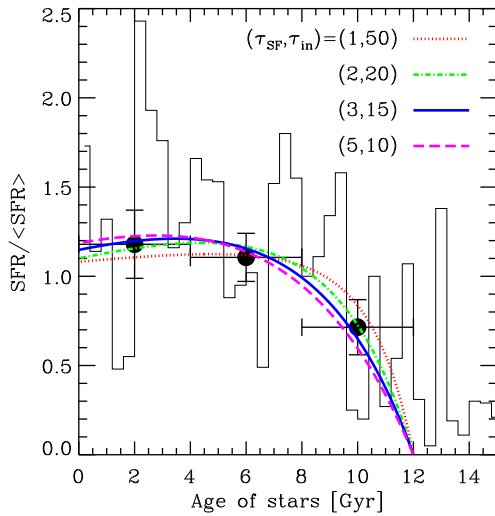


Fig. 4. Star formation history (time evolution of star formation rate) normalized by the average rate. The histogram is the observed history at the solar neighborhood reported by Rocha-Pinto et al. (2000a). The filled circles with error-bars are the average of the histogram over 4 Gyr interval and corrected by the average rate only for the age less than 12 Gyr which is the present age of the Milky Way assumed in this paper. The vertical error-bars are the standard error of the mean. The four lines correspond to the time evolutions with four different sets of time-scales of star formation and infall ($\tau_{\text{SF}}/\text{Gyr}$, $\tau_{\text{in}}/\text{Gyr}$) as indicated in the panel.

densation of metal elements. In Figure 3, we show three cases of $\xi = 1$ (all metal condenses into dust: an extreme but unrealistic case), 0.1 (fiducial case), and 0.01 (a lower efficiency case). The reader may be anxious about a large uncertainty of this approximation. However, the dust mass in galaxies does not depend on m_d after the accretion growth becomes active. This is because the growth of dust is the dominant process of dust production after the activation as shown later in §6.1.

4. Milky Way analog

Let us calibrate parameters in the chemical and dust evolution model of galaxies so as to reproduce the properties at the solar neighborhood in the Milky Way. There are two parameters in the chemical evolution part: the time-scales of star formation, τ_{SF} , and infall, τ_{in} . There are additional two parameters in the dust content evolution: the time-scale of the ISM accretion growth, $\tau_{\text{ac},0}$, and the efficiency of the dust destruction, ϵm_{SN} . In addition, there are two parameters as uncertainties of metal and dust yields, f_Z and ξ . Table 1 is a summary of these parameters and values.

Note that we do not apply any statistical method to justify the goodness of the reproduction of the observational constraints throughout this paper because our aim is not to find the best fit solution for the constraints but to demonstrate the dust content evolution in galaxies qualitatively. This is partly due to the weakness of the observational constraints and due to large uncertainties of the dust physics itself.

4.1 Chemical evolution at the solar neighborhood

We here determine the time-scales of star formation and infall in the chemical evolution part. First, we constrain these time-scales by using the star formation history at the solar neighborhood reported by Rocha-Pinto et al. (2000a).

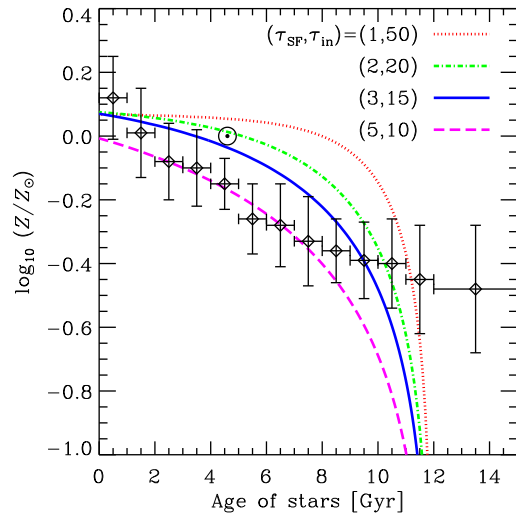


Fig. 5. Age-metallicity relation of stars. The diamonds with error-bars are the data of stars at the solar neighborhood reported by Rocha-Pinto et al. (2000b). The solar mark (\odot) indicates the position of the Sun on this plot. The four lines correspond to the model relations same as Fig. 4. The present age of the Milky Way is assumed to be 12 Gyr.

Such a method was adopted by Takeuchi & Hirashita (2000). Rocha-Pinto et al. (2000a) derived the star formation history from the age distribution of 552 late-type dwarf stars at the solar neighborhood. The histogram in Figure 4 is their result and shows very stochastic nature of the history. However, our model can treat only a smooth history. Thus, we smoothed the stochastic history by averaging with 4 Gyr interval. The filled circles are the result. The vertical error-bars indicate the standard error of the mean. The average history is re-normalized by the average star formation rate for the stellar age less than 12 Gyr which is the assumed age of the Milky Way in this paper, although this choice of the age is arbitrary. We have tried four cases of τ_{SF} in this paper: 1, 2, 3, and 5 Gyr which are the observed range of the time-scale (or gas consumption time-scale) for disk galaxies like the Milky Way (e.g., Larson, Tinsley, & Caldwell 1980). For each τ_{SF} , we have found τ_{in} with which we can reproduce the smoothed history as shown in Figure 4.

Next, we adopt the observed relation between the stellar age and metallicity, so-called the age-metallicity relation, reported by Rocha-Pinto et al. (2000b) to further constrain ($\tau_{\text{SF}}, \tau_{\text{in}}$). Rocha-Pinto et al. (2000b) derived the relation from the same 552 stars as Rocha-Pinto et al. (2000a). Their result is shown in Figure 5 by diamonds with error-bars. After comparing with our four model lines, we have found that ($\tau_{\text{SF}}/\text{Gyr}, \tau_{\text{in}}/\text{Gyr}$) = (5, 10) case seems the best match with the observed relation but ($\tau_{\text{SF}}/\text{Gyr}, \tau_{\text{in}}/\text{Gyr}$) = (3, 15) case is also acceptable.

Finally, we adopt another constraint: the current stellar mass relative to the ISM mass. Naab & Ostriker (2006) compiled observational constraints for the solar neighborhood. From the compilation, we adopt the ratio of the stellar mass to the ISM mass at the present epoch of 3.1 ± 1.4 . Note that the stellar mass includes the remnant mass (i.e. white dwarf, neutron stars, and black-holes). Figure 6 shows the comparison of the ratio with our four star formation histories.

Table 1. Parameters and values for the solar neighborhood.

Parameter	Fiducial value	Considered values
$(\tau_{\text{SF}}/\text{Gyr}, \tau_{\text{in}}/\text{Gyr})$	(3, 15)	(1, 50), (2, 20), (3, 15), and (5, 10)
$(\tau_{\text{ac},0}/\text{Myr}, \epsilon m_{\text{SN}}/10^3 M_{\odot})$	(3, 1)	(1.5, 1), (1.5, 2), (3, 0.5), (3, 1), (3, 2), (6, 0.5), and (6, 1)
f_Z	0.02	0.01, 0.02, and 0.04
ξ	0.1	0.01, 0.1, and 1

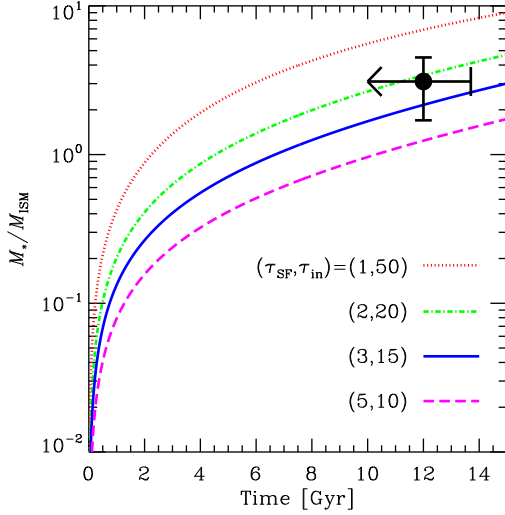


Fig. 6. Time evolution of the stellar mass relative to the ISM mass. The filled circle with error-bars is an estimate at the solar neighborhood taken from Naab & Ostriker (2006) and references therein. Note that the stellar mass includes mass of remnants. The present age of the Milky Way should be less than the age of the Universe (13.7 Gyr). The four lines correspond to the model evolutions same as Fig. 4.

We have found that the two sets of $(\tau_{\text{SF}}/\text{Gyr}, \tau_{\text{in}}/\text{Gyr}) = (2, 20)$ and $(3, 15)$ are consistent with the data.

From these three comparisons, we finally adopt the case of $(\tau_{\text{SF}}/\text{Gyr}, \tau_{\text{in}}/\text{Gyr}) = (3, 15)$ as the fiducial set for the Milky Way (or more precisely, for the solar neighborhood) in this paper.

4.2 Dust content evolution at the solar neighborhood

Here we examine the dust content evolution. First, we show the significant effect of the dust destruction and the ISM growth. Figure 7 shows the time evolution of metallicity and dust-to-gas mass ratio for the fiducial set of τ_{SF} and τ_{in} obtained in the previous subsection. The model curves of the dust-to-gas ratio (dotted, dot-dashed, and solid lines) are compared with the filled circle with error-bars which is an observational estimate at the solar neighborhood. This is obtained from metallicity $Z \approx Z_{\odot}$ (van den Bergh 2000; see also Rocha-Pinto et al. 2000b) and dust-to-metal mass ratio $\delta \approx 0.5$ (Kimura et al. 2003; see below) and the uncertainty is the quadrature of uncertainties of 30%⁵ in Z and 20% in δ .

If there is neither destruction nor accretion growth of dust, the dust-to-gas ratio evolution is just the metallicity evolution multiplied by the condensation efficiency of stardust, ξ , as

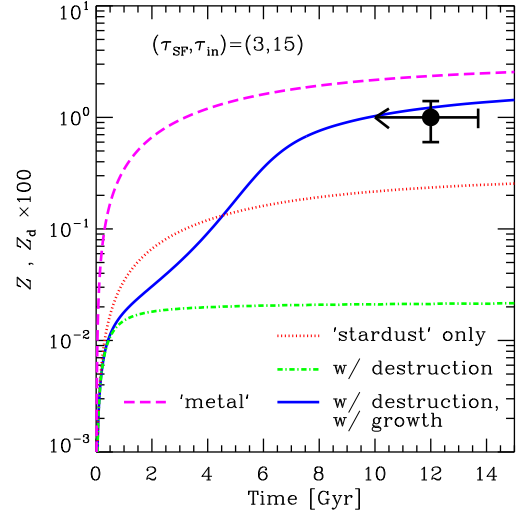


Fig. 7. Time evolution of metallicity (metal mass fraction in the ISM; dashed line) and dust-to-gas mass ratio (other lines) for the fiducial case (Table 1). The dotted line corresponds to the case only with ‘stardust’ production and destruction by star formation (i.e. astration). The dot-dashed line correspond to the case with the dust destruction by SNe but without the dust growth in the ISM. The solid line is the case with all the processes. The filled circle with error-bars is an estimate of the dust-to-gas mass ratio at the solar neighborhood (see text). The present age of the Milky Way should be less than the age of the Universe (13.7 Gyr).

shown by the dotted line. We have assumed $\xi = 0.1$ for the line. Once the SN destruction of dust is turned on with a standard efficiency as $\epsilon m_{\text{SN}} = 1 \times 10^3 M_{\odot}$ (McKee 1989; Nozawa et al. 2006), it reduces the dust amount by a factor of ten as shown by the dot-dashed line. This confirms that the dust destruction is very efficient and the stardust injection is too small to compensate the destruction (e.g., Draine 1990; Tielens 1998). Then we need the accretion growth in the ISM to reproduce the dust-to-gas ratio $\sim 10^{-2}$ in the present Milky Way. If we assume the time-scale of $\tau_{\text{ac},0} = 3 \times 10^6$ yr, the dust-to-gas ratio evolution becomes the solid line and it reaches $\sim 10^{-2}$ which is almost two orders of magnitude larger than the case without the growth after several Gyr.

Figure 8 shows the time evolution of τ_{SN} in equation (13) and τ_{ac} in equation (17). The SN destruction time-scale τ_{SN} is almost constant promptly after the first a few hundreds Myr. On the other hand, the accretion growth time-scale τ_{ac} decreases gradually in the first a few Gyr. This is because τ_{ac} has a metallicity dependence as shown in equation (17) and it decreases as the metallicity increases. At the time around 4 Gyr, τ_{ac} becomes shorter than τ_{SN} , and then, the accretion growth becomes significant and the dust amount increases rapidly. As the accretion growth proceeds, the

⁵The difference between Z_{\odot} by Anders & Grevesse (1989) and Asplund et al. (2009) accounts for the uncertainty.

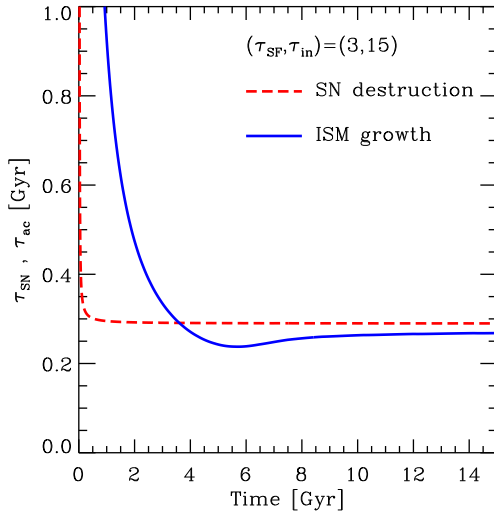


Fig. 8. Time evolution of time-scales of the dust destruction by SNe (dashed line) and of the dust growth in the ISM (solid line) for the fiducial case (Table 1).

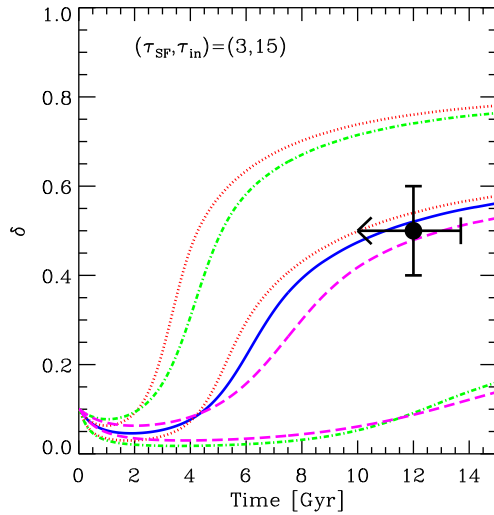


Fig. 9. Time evolution of dust-to-metal mass ratio, δ , for various sets of the parameters of dust growth and destruction ($\tau_{\text{ac},0}, \epsilon m_{\text{SN}}$). The solid line is the fiducial case with (3×10^6 yr, $1 \times 10^3 M_{\odot}$). The two dotted lines correspond to two different sets of (1.5×10^6 yr, $1 \times 10^3 M_{\odot}$) for the upper and (1.5×10^6 yr, $2 \times 10^3 M_{\odot}$) for the lower. The two dot-dashed lines correspond to the sets of (3×10^6 yr, $5 \times 10^2 M_{\odot}$) for the upper and (3×10^6 yr, $2 \times 10^3 M_{\odot}$) for the lower. The two dashed lines correspond to the sets of (6×10^6 yr, $5 \times 10^2 M_{\odot}$) for the upper and (6×10^6 yr, $1 \times 10^3 M_{\odot}$) for the lower. The filled circle with error-bars is an estimate in the Local Interstellar Cloud surrounding the Sun by Kimura et al. (2003). The present age of the Milky Way should be less than the age of the Universe (13.7 Gyr).

metal abundance in the gas phase decreases, i.e., the dust-to-metal ratio δ increases, then, τ_{ac} becomes almost constant and balances with τ_{SN} . We will discuss this point in §5 more in detail.

Figure 9 shows the time evolution of the dust-to-metal ratio, δ . The solid line is the fiducial case which is shown in Figures 7 and 8. This can be compared with the observed ratio in the Local Interstellar Cloud reported by Kimura et al. (2003): $\delta = 0.5 \pm 0.1$. As shown in Figure 9, the fidu-

cial set of $(\tau_{\text{ac},0}, \epsilon m_{\text{SN}}) = (3 \text{ Myr}, 1 \times 10^3 M_{\odot})$ excellently agrees with the observed data. On the other hand, other sets can also reproduce the data. For example, $(\tau_{\text{ac},0}, \epsilon m_{\text{SN}}) = (1.5 \text{ Myr}, 2 \times 10^3 M_{\odot})$ or $(6 \text{ Myr}, 5 \times 10^2 M_{\odot})$. Interestingly, the δ evolutions become very similar if the product of $\tau_{\text{ac},0}$ and ϵm_{SN} is the same. We will also discuss this point in §5.

5. Determining dust-to-metal ratio

In this section, we demonstrate the mechanism for determining the dust-to-metal mass ratio, δ , in galaxies. Starting from equations (3) and (4), we can obtain the time evolutionary equation of $\delta \equiv M_{\text{d}}/M_{\text{Z}}$. Here, let us adopt the instantaneous recycling approximation (IRA) in which we neglect the finite stellar life-time and assume that stars with a mass larger than a certain threshold (the turn-off mass m_t) die instantly when they are formed. This approximation allows us to manage the equations analytically and is good enough to see phenomena with a time-scale longer than a Gyr (see Tinsley 1980 for more details). In the IRA, we can approximate the metal and dust yields in equations (10) and (11) as $Y_{\text{Z}} \approx \mathcal{Y}_{\text{Z}} S$ and $Y_{\text{d}} = \xi Y_{\text{Z}} \approx \xi \mathcal{Y}_{\text{Z}} S$, where the effective metal yield

$$\mathcal{Y}_{\text{Z}} = \int_{m_t}^{m_{\text{up}}} m_{\text{Z}}(m) \phi(m) dm = 0.024 \left(\frac{f_{\text{Z}}}{0.02} \right), \quad (22)$$

where we have assumed $m_t = 1 M_{\odot}$. This value is not sensitive to m_t . We obtain $\mathcal{Y}_{\text{Z}} = 0.021 (f_{\text{Z}}/0.02)$ if $m_t = 5 M_{\odot}$. Remembering the star formation rate $S = M_{\text{ISM}}/\tau_{\text{SF}}$ as in equation (5), then, we obtain

$$\frac{1}{\delta} \frac{d\delta}{dt} \approx -\frac{\mathcal{Y}_{\text{Z}}}{\tau_{\text{SF}} Z} \left(1 - \frac{\xi}{\delta} \right) - \frac{1}{\tau_{\text{SN}}} - \frac{1}{\tau_{\text{ac}}}. \quad (23)$$

In the IRA, the SN destruction time-scale τ_{SN} in equation (13) can be reduced to

$$\tau_{\text{SN}} \approx \frac{\tau_{\text{SF}}}{\epsilon m_{\text{SN}} n_{\text{SN}}}, \quad (24)$$

where the effective number of SN per unit stellar mass is

$$n_{\text{SN}} = \int_{8M_{\odot}}^{40M_{\odot}} \phi(m) dm = 0.010 M_{\odot}^{-1}. \quad (25)$$

Note that $\epsilon m_{\text{SN}} n_{\text{SN}}$ is a non-dimensional value. The accretion growth time-scale τ_{ac} is given in equation (17). Then, equation (23) is reduced to

$$\frac{1}{\delta} \frac{d\delta}{dt} \approx -\frac{\alpha + \epsilon m_{\text{SN}} n_{\text{SN}}}{\tau_{\text{SF}}} + \frac{Z(1-\delta)}{\tau_{\text{ac},0}}, \quad (26)$$

where

$$\alpha = \frac{\mathcal{Y}_{\text{Z}}}{Z} \left(1 - \frac{\xi}{\delta} \right). \quad (27)$$

In the IRA, the metallicity $Z \equiv M_{\text{Z}}/M_{\text{ISM}}$ can be obtained analytically (for example, see Dwek et al. 2007). Then, we have found that $Z \rightarrow \mathcal{Y}_{\text{Z}}$ for $t \rightarrow \infty$ when $\tau_{\text{in}} > \tau_{\text{SF}}$. The condensation efficiency ξ is uncertain but it is of the order of 0.1 (see Figure 3). When δ is of the order of 0.1–1 as shown in Figure 9, the ratio ξ/δ is of the order of

1 or smaller. Therefore, α is also of the order of 1 or smaller. On the other hand, $n_{\text{SN}} \sim 10^{-2} M_{\odot}^{-1}$ and $\epsilon m_{\text{SN}} \sim 10^3 M_{\odot}$, then, we obtain $\epsilon m_{\text{SN}} n_{\text{SN}} \gg \alpha$. Therefore, equation (26) is further reduced to

$$\frac{1}{\delta} \frac{d\delta}{dt} \approx -a + b(1 - \delta), \quad (28)$$

where $a = \epsilon m_{\text{SN}} n_{\text{SN}} / \tau_{\text{SF}}$ and $b = Z / \tau_{\text{ac},0}$. If we assume Z to be constant (i.e. b is constant), equation (28) can be solved analytically. The solution is

$$\delta \approx \frac{\delta_{\infty} \delta_0 \exp(b - a)t}{(\delta_{\infty} - \delta_0) + \delta_0 \exp(b - a)t}, \quad (29)$$

where δ_0 and δ_{∞} are the values for $t = 0$ and $t \rightarrow \infty$, respectively. The asymptotic value δ_{∞} for $t \rightarrow \infty$ is realized only when $b > a$, and is given by

$$1 - \delta_{\infty} = \frac{a}{b} = \frac{\tau_{\text{ac},0} \epsilon m_{\text{SN}} n_{\text{SN}}}{\tau_{\text{SF}} Z}. \quad (30)$$

This is the equilibrium value for equation (28) and we find

$$1 - \delta_{\infty} = 0.5 \left(\frac{\tau_{\text{ac},0}}{3 \text{ Myr}} \right) \left(\frac{\epsilon m_{\text{SN}}}{10^3 M_{\odot}} \right) \left(\frac{n_{\text{SN}}}{10^{-2} M_{\odot}^{-1}} \right) \times \left(\frac{3 \text{ Gyr}}{\tau_{\text{SF}}} \right) \left(\frac{0.02}{Z} \right) \quad (31)$$

which excellently agrees with the results in Figure 9.

We can fully understand the δ evolution by using equation (28). At the beginning, the accretion term $b \sim 0$ because $Z \sim 0$. Then, only the destruction term a is effective. As a result, δ decreases with the time-scale of $1/a = \tau_{\text{SN}}$. As Z increases, the accretion term b increases and finally exceeds a . Then, δ increases toward δ_{∞} with the evolution time-scale of $1/(b - a)$. This decreases as Z increases and $b - a$ increases. Therefore, the driving force of the δ evolution is Z . If we call Z at $b = a$ as the critical metallicity, Z_c , we find

$$Z_c = \frac{\tau_{\text{ac},0} \epsilon m_{\text{SN}} n_{\text{SN}}}{\tau_{\text{SF}}} = 0.01 \times \left(\frac{\tau_{\text{ac},0}}{3 \text{ Myr}} \right) \left(\frac{\epsilon m_{\text{SN}}}{10^3 M_{\odot}} \right) \left(\frac{n_{\text{SN}}}{10^{-2} M_{\odot}^{-1}} \right) \left(\frac{3 \text{ Gyr}}{\tau_{\text{SF}}} \right) \quad (32)$$

When $Z > Z_c$, the accretion growth becomes effective and δ approaches the final value δ_{∞} . A similar critical metallicity has been derived by Asano et al. (2011) with a different way.

Equation (30) shows that the final value of δ is determined by the equilibrium between the SN destruction and the accretion growth in the ISM. The time-scale to reach the equilibrium is $1/(b - a)$. This is relatively short in the fiducial case. For example, it is 0.3 Gyr when $Z = 0.02$. This means that the δ evolution proceeds with keeping the equilibrium between the SN destruction and the accretion growth, or equivalently, $\delta = \delta_{\infty}$ after Z exceeds Z_c . This behavior is also found by the comparison of the two time-scales, τ_{SN} and τ_{ac} , in Figure 8; once τ_{ac} becomes shorter than τ_{SN} at about 4 Gyr at which Z exceeds Z_c , τ_{ac} turns around and approaches τ_{SN} again. This is realized by the reduction of the term $(1 - \delta)$ in τ_{ac} (see eq. [17]) when δ increases from ~ 0 to δ_{∞} . Such a kind of self-regulation process determines the dust-to-metal ratio δ .

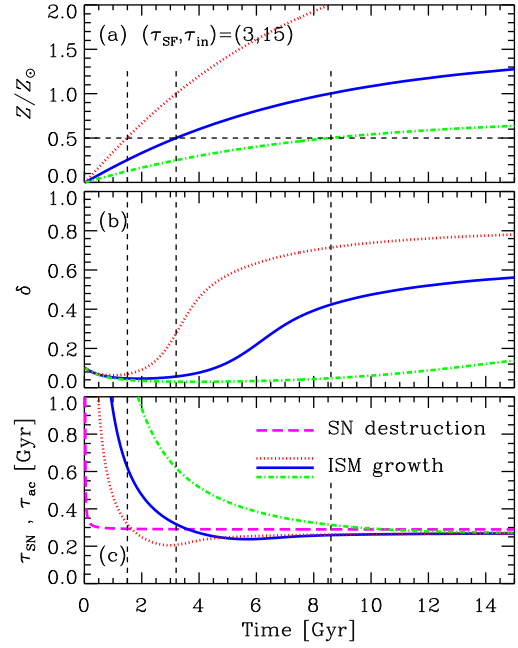


Fig. 10. Time evolution of (a) metallicity, (b) dust-to-metal mass ratio, and (c) time-scales of SN destruction and ISM growth for three different stellar metal yields: $f_Z = 0.01$ (dot-dashed), 0.02 (solid), and 0.04 (dotted). The horizontal short-dashed line in the panel (a) shows the critical metallicity of equation (32). The vertical short-dashed lines indicate the timing at which the metallicity exceeds the critical one for the three metal yields. The long-dashed line in the panel (c) is the SN destruction time-scale, but the other three lines are the ISM growth time-scales for the three metal yields.

6. Discussion

6.1 Effect of uncertainties of yields

Here we examine the effect of uncertainties of the normalization of metal and dust yields. As we saw in Figure 2, our simple recipe for the metal yield may contain a factor of 2 (or more) uncertainty. The parameter f_Z accounts for this uncertainty. In Figure 10, we show the effect of f_Z . As found from the panel (a), the metallicity evolution is scaled almost linearly by f_Z as expected and the timing at which Z exceeds $Z_c = 0.5 Z_{\odot}$ given by equation (32) for the fiducial set of the accretion and destruction efficiencies becomes faster as f_Z is larger. From the panels (b) and (c), we find that for each case of f_Z , δ increases and τ_{ac} becomes shorter than τ_{SN} soon after the timing for $Z > Z_c$. Therefore, the timing for $\tau_{\text{ac}} < \tau_{\text{SN}}$, in other words, the timing for the accretion growth activation is well traced by Z_c in equation (32) and this is not affected by uncertainty of f_Z . On the other hand, the timing for the activation becomes faster for larger f_Z . The metallicity dependence on the final value of δ is explicit as found in equation (31).

Figure 11 shows the effect of the dust yield. As seen in Figure 3, our recipe for the stardust yield has a factor of 10 or larger uncertainty because of a large uncertainty in the adopted model calculations. In Figure 11, we show the cases with a factor of 10 larger or smaller yield than the fiducial one. Other parameters are the same as the fiducial set, so that we have the same evolutions of the metallicity and the time-scales of the SN destruction and accretion growth as shown by the solid lines in Figure 10. Before the growth

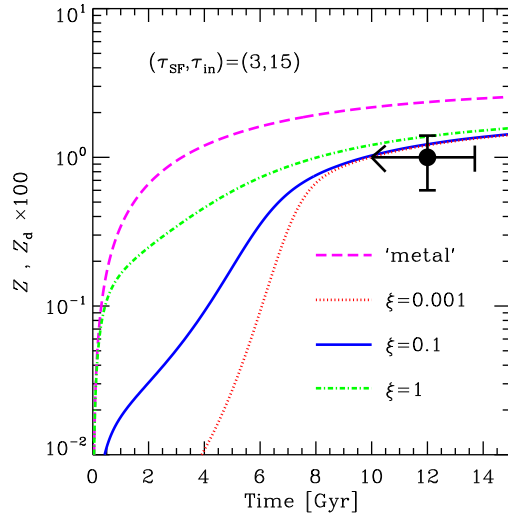


Fig. 11. Same as Fig. 7 but for different condensation efficiencies in the stellar ejecta as indicated in the panel.

activation at around 4 Gyr, the dust amounts show a large difference, however, they converge nearly the same amount after the activation. This is because the final value of δ given in equation (31) does not depend on the dust yield. Therefore, we conclude that the dust content in galaxies is independent of the stardust yield after the grain growth in the ISM becomes active, or equivalently, the metallicity exceeds the critical one.

6.2 What kind of dust is formed by the ISM growth?

We have shown that the main production channel of dust is the accretion growth in the ISM of the present-day Milky Way. This conclusion had been obtained also in the literature. For example, Zhukovska et al. (2008) argued that the mass fraction of stardusts in total dust is only 0.1–1% based on a more sophisticated chemical evolution model than this paper (see their Fig. 15); more than 99% of dust is originated from the accretion growth in the ISM. It is also well known that some interplanetary dust particles show a highly enhanced abundance of deuterium and ^{15}N relative to the solar composition, which is a signature of the molecular cloud origin because such isotopic fractionations are expected in low temperature environment (e.g., Messenger 2000). Therefore, dust produced by the ISM accretion exists. Then, we have a very important question; what kinds of dust species are formed by the accretion growth in the ISM?

In molecular clouds, many kinds of ices such as H_2O , CO , CO_2 , CH_3OH have been detected (e.g., Gibb et al. 2000). These ices are condensed onto pre-existent grains. In these ices, some chemical reactions and ultraviolet photolysis (and cosmic rays) process the material and may make it refractory. As a result, so-called ‘core-mantle grains’ coated by refractory organics would be formed (e.g., Li & Greenberg 1997). Indeed, such a grain has been found in cometary dust: olivine particles produced by a Type II SN coated by organic matter which seems to be formed in a cold molecular cloud (Messenger et al. 2005). Therefore, the ISM dust probably has core-mantle or layered structures. Moreover, the composition can be heterogeneous: for example, graphite coated

by silicate, silicate coated by graphite, silicate coated by iron, etc. The formation of such grains does not seem to be studied well. Much more experimental and theoretical works are highly encouraged.

If we can find signatures of the dust accretion growth in the ISM of galaxies by astronomical observations (i.e. very distant remote-sensing), it proves the growth ubiquitous. A possible evidence already obtained is a huge mass of dust in galaxies which requires the accretion growth as discussed in this paper. It is worth studying how to distinguish stardust grains (or grain cores) and ISM dust (or mantle) by observations, e.g., spectropolarimetry, in future.

6.3 Dust amount in the proto-solar nebula

We have shown that the dust amount is very small before the ISM growth becomes active. For example, the dust-to-gas mass ratio is of the order of 10^{-4} at the first a few Gyr from the formation of the Milky Way (or the onset of the major star formation at the solar neighborhood). If the dust-to-gas ratio in the proto-solar nebula was 10^{-4} , the planet formation might be difficult. Fortunately, the activation of the ISM growth is expected to be about 8 Gyr ago at the solar neighborhood. Thus, it is well before the solar system formation. Indeed, we expect the dust-to-gas ratio of several times 10^{-3} at 4–5 Gyr ago (see Figure 7). Moreover, the dust-to-gas ratio may be much enhanced in the proto-solar nebula relative to the average ISM. This is because the accretion growth is more efficient for higher density and the density in the proto-solar nebula is several orders of magnitude higher than that in molecular clouds. Therefore, even if the solar system formation is before the activation of the ISM growth globally, the dust growth may be active locally in the proto-solar nebula. In this case, the planet formation is always possible if there is enough metal to accrete onto the pre-existent seed grains, even before the global growth activation. This is an interesting issue to relate to the Galactic Habitable Zone where complex life can be formed (Lineweaver et al. 2004). We will investigate it more in future.

Acknowledgments. The author thanks to anonymous referees for their many suggestions which were useful to improve the presentation and the quality of this paper. The author is grateful to T. Kozasa and A. Habe for interesting discussions and for their hospitality during my stay in Hokkaido University, Sapporo where this work was initiated, to R. Asano, H. Hirashita, and T. T. Takeuchi for many discussions, to T. Nozawa for providing his dust yields in SNe, and to H. Kimura, the chair of the convener of the ‘Cosmic Dust’ session in the AOGS 2010 meeting, for inviting me to the interesting meeting in Hyderabad, India. This work is supported by KAKENHI (the Grant-in-Aid for Young Scientists B: 19740108) by The Ministry of Education, Culture, Sports, Science and Technology (MEXT) of Japan.

References

- Anders, E., Grevesse, N., Abundances of the elements - Meteoritic and solar, *Geochim. Cosmochim. Acta.*, **53**, 197–214, 1989.
- Arendt, R. G., Dwek, E., Petre, R., An infrared analysis of Puppis A, *Astrophys. J.*, **368**, 474–485, 1991.
- Arendt, R. G., Dwek, E., Blair, W. P., Ghavamian, P., Hwang, U., Long, K. S., Petre, R., Rho, J., Winkler, P. F., Spitzer Observations of Dust Destruction in the Puppis A Supernova Remnant, *Astrophys. J.*, **725**, 585–597, 2010.
- Asano, R., Takeuchi, T. T., Hirashita, H., Inoue, A. K., Dust formation history of galaxies: metallicity vs. grain growth, *Astron. Astrophys.*, submitted.

- Asplund, M., Grevesse, N., Sauval, A. J., Scott, P., The Chemical Composition of the Sun, *Ann. Rev. Astron. Astrophys.*, **47**, 481–522, 2009.
- Barlow, M. J., Krause, O., Swinyard, B. M., Sibthorpe, B., Besel, M.-A., Wesson, R., Ivison, R. J., Dunne, L., et al., A Herschel PACS and SPIRE study of the dust content of the Cassiopeia A supernova remnant, *Astron. Astrophys.*, **518**, L138, 2010.
- Bertelli, G., Bressan, A., Chiosi, C., Fagotto, F., Nasi, E., Theoretical isochrones from models with new radiative opacities, *Astron. Astrophys. Suppl.*, **106**, 275–302, 1994.
- Bianchi, S., Ferrara, A., Intergalactic medium metal enrichment through dust sputtering, *M.N.R.A.S.*, **358**, 379–396, 2005.
- Bianchi, S., Schneider, R., Dust formation and survival in supernova ejecta, *M.N.R.A.S.*, **378**, 973–982, 2007.
- Borkowski, K. J., Williams, B. J., Reynolds, S. P., Blair, W. P., Ghavamian, P., Sankrit, R., Hendrick, S. P., Long, K. S., et al., Dust Destruction in Type Ia Supernova Remnants in the Large Magellanic Cloud, *Astrophys. J.*, **642**, L141–L144, 2006.
- Calura, F., Pipino, A., Matteucci, F., The cycle of interstellar dust in galaxies of different morphological types, *Astron. Astrophys.*, **479**, 669–685, 2008.
- Chabrier, G., Galactic Stellar and Substellar Initial Mass Function, *Publ. Astron. Soc. Pac.*, **115**, 763–795, 2003.
- Dopita, M. A., Ryder, S. D., On the law of star formation in disk galaxies, *Astrophys. J.*, **430**, 163–178, 1996.
- Draine, B. T., Evolution of interstellar dust, in *The evolution of the interstellar medium*, 13 pp, Astronomical Society of the Pacific, San Francisco, 1990.
- Draine, B. T., Interstellar Dust Models and Evolutionary Implications, in *Cosmic Dust - Near and Far*, Edited by Henning, T., Grün, E., Steinacker, J., 20 pp, Astronomical Society of the Pacific, San Francisco, 2009.
- Draine, B. T., Salpeter, E. E., Time-dependent nucleation theory, *J. of Chem. Phys.*, **67**, 2230–2235, 1977.
- Draine, B. T., Salpeter, E. E., Destruction mechanisms for interstellar dust, *Astrophys. J.*, **231**, 438–455, 1979.
- Dunne, L., Eales, S., Ivison, R., Morgan, H., Edmunds, M., Type II supernovae as a significant source of interstellar dust, *Nature*, **424**, 285–287, 2003.
- Dunne, L., Maddox, S. J., Ivison, R. J., Rudnick, L., Delaney, T. A., Matthews, B. C., Crowe, C. M., Gomez, H. L., Eales, S. A., Dye, S., Cassiopeia A: dust factory revealed via submillimetre polarimetry, *M.N.R.A.S.*, **394**, 1307–1316, 2009.
- Dwek, E., The Evolution of the Elemental Abundances in the Gas and Dust Phases of the Galaxy, *Astrophys. J.*, **501**, 643–665, 1998.
- Dwek, E., Scalo, J. M., The evolution of refractory interstellar grains in the solar neighborhood, *Astrophys. J.*, **239**, 193–211, 1980.
- Dwek, E., Arendt, R. G., Dust-gas interactions and the infrared emission from hot astrophysical plasmas, *Ann. Rev. Astron. Astrophys.*, **30**, 11–50, 1992.
- Dwek, E., Galliano, F., Jones, A. P., The Evolution of Dust in the Early Universe with Applications to the Galaxy SDSS J1148+5251, *Astrophys. J.*, **662**, 927–939, 2007.
- Dwek, E., Arendt, R. G., Bouchet, P., Burrows, D. N., Challis, P., Danziger, I. J., De Buizer, J. M., Gehrz, R. D., et al., Infrared and X-Ray Evidence for Circumstellar Grain Destruction by the Blast Wave of Supernova 1987A, *Astrophys. J.*, **676**, 1029–1039, 2008.
- Dwek, E., Cherchneff, I., The Origin of Dust in the Early Universe: Probing the Star Formation History of Galaxies by Their Dust Content, *Astrophys. J.*, **727**, 63, 2011.
- Edmunds, M. G., An elementary model for the dust cycle in galaxies, *M.N.R.A.S.*, **328**, 223–236, 2003.
- Edmunds, M. G., Eales, S. A., Maximum dust masses in galaxies, *M.N.R.A.S.*, **299**, L29–L31, 1998.
- Elmegreen, B. G., Star Formation on Galactic Scales: Empirical Laws, in *Ecole Evry Schatzman 2010: Star Formation in the Local Universe. Lecture 1 of 5*, 2011. (arXiv:1101.3108)
- Ferrarotti, A. S., Gail, H.-P., Composition and quantities of dust produced by AGB-stars and returned to the interstellar medium, *Astron. Astrophys.*, **447**, 553–576, 2006.
- Gall, C., Andersen, A. C., Hjorth, J., Genesis and evolution of dust in galaxies in the early Universe I. Modeling dust evolution in starburst galaxies, *Astron. Astrophys.*, in press (arXiv:1011.3157)
- Gall, C., Andersen, A. C., Hjorth, J., Genesis and evolution of dust in galaxies in the early Universe II. Rapid dust evolution in quasars at $z > 6$, *Astron. Astrophys.*, in press (arXiv:1101.1553)
- Gehrz, R., Sources of Stardust in the Galaxy, in *Interstellar Dust*, Edited by Allamandola, L. J. and Tielens, A. G. G. M., 445 pp, International Astronomical Union. Symposium no. 135, Kluwer Academic Publishers, Dordrecht, 1989
- Gibb, E. L., et al., An Inventory of Interstellar Ices toward the Embedded Protostar W33A, *Astrophys. J.*, **536**, 347–356, 2000.
- Gomez, H. L., Dunne, L., Ivison, R. J., Reynoso, E. M., Thompson, M. A., Sibthorpe, B., Eales, S. A., Delaney, T. M., Maddox, S., Isaak, K., Accounting for the foreground contribution to the dust emission towards Kepler's supernova remnant, *M.N.R.A.S.*, **397**, 1621–1632, 2009.
- Heger, A., Fryer, C. L., Woosley, S. E., Langer, N., Hartmann, D. H., How Massive Single Stars End Their Life, *Astrophys. J.*, **591**, 288–300, 2003.
- Hirashita, H., Global Law for the Dust-to-Gas Ratio of Spiral Galaxies, *Astrophys. J.*, **510**, L99–L102, 1999a.
- Hirashita, H., Dust-to-gas ratio and phase transition of interstellar medium, *Astron. Astrophys.*, **344**, L87–L89, 1999b.
- Hirashita, H., Dust-to-Gas Ratio and Metallicity in Dwarf Galaxies, *Astrophys. J.*, **522**, 220–224, 1999c.
- Hirashita, H., Cyclic Changes in Dust-to-Gas Ratio, *Astrophys. J.*, **531**, 693–700, 2000a.
- Hirashita, H., Dust Growth Timescale and Mass Function of Molecular Clouds in the Galaxy, *Publ. Astron. Soc. Jpn.*, **52**, 585–588, 2000b.
- Hirashita, H., Effects of grain size distribution on the interstellar dust mass growth, *M.N.R.A.S.*, submitted.
- Hirashita, H., Tajiri, Y. Y., Kamaya, H., Dust-to-gas ratio and star formation history of blue compact dwarf galaxies, *Astron. Astrophys.*, **388**, 439–445, 2002.
- Ikeuchi, S., Tomita, H., Cyclic phase changes of interstellar medium, *Publ. Astron. Soc. J.*, **35**, 77–86, 1983.
- Inoue, A. K., Evolution of Dust-to-Metal Ratio in Galaxies, *Publ. Astron. Soc. Jpn.*, **55**, 901–909, 2003.
- Inoue, A. K., Kamaya, H., Constraint on intergalactic dust from thermal history of intergalactic medium, *M.N.R.A.S.*, **341**, L7–L11, 2003.
- Inoue, A. K., Kamaya, H., Amount of intergalactic dust: constraints from distant supernovae and the thermal history of the intergalactic medium, *M.N.R.A.S.*, **350**, 729–744, 2004.
- Inoue, A. K., Kamaya, H., Intergalactic dust and its photoelectric heating, *Earth, Planets, Space*, **62**, 69–79, 2010.
- Iwamoto, K., Brachwitz, F., Nomoto, K., Kishimoto, N., Umeda, H., Hix, W. R., Thielemann, F.-K., Nucleosynthesis in Chandrasekhar Mass Models for Type IA Supernovae and Constraints on Progenitor Systems and Burning-Front Propagation, *Astrophys. J. Suppl.*, **125**, 439–462, 1999.
- Jenkins, E. B., A Unified Representation of Gas-Phase Element Depletions in the Interstellar Medium, *Astrophys. J.*, **700**, 1299–1348, 2009.
- Jones, A. P., Tielens, A. G. G. M., Hollenbach, D. J., McKee, C. F., Grain destruction in shocks in the interstellar medium, *Astrophys. J.*, **433**, 797–810, 1994.
- Jones, A. P., Tielens, A. G. G. M., Hollenbach, D. J., Grain Shattering in Shocks: The Interstellar Grain Size Distribution, *Astrophys. J.*, **469**, 740–764, 1996.
- Karakas, A. I., Updated stellar yields from asymptotic giant branch models, *M.N.R.A.S.*, **403**, 1413–1425, 2010.
- Kennicutt, R. C., The Global Schmidt Law in Star-forming Galaxies, *Astrophys. J.*, **498**, 541–552, 1998.
- Kimura, H., Mann, I., Jessberger, E. K., Composition, Structure, and Size Distribution of Dust in the Local Interstellar Cloud, *Astrophys. J.*, **583**, 314–321, 2003.
- Kozasa, T., Hasegawa, H., Grain Formation through Nucleation Process in Astrophysical Environments. II —Nucleation and Grain Growth Accompanied by Chemical Reaction—, *Progress of Theoretical Physics*, **77**, 1402–1410, 1987.
- Kozasa, T., Nozawa, T., Tominaga, N., Umeda, H., Maeda, K., Nomoto, K., Dust in Supernovae: Formation and Evolution, in *Cosmic Dust - Near and Far*, Edited by Henning, T., Grün, E., Steinacker, J., 43 pp, Astronomical Society of the Pacific, San Francisco, 2009.
- Krause, O., Birkmann, S. M., Rieke, G. H., Lemke, D., Klaas, U., Hines, D. C., Gordon, K. D., No cold dust within the supernova remnant Cassiopeia A, *Nature*, **432**, 596–598, 2004.
- Kroupa, P., The Initial Mass Function of Stars: Evidence for Uniformity in Variable Systems, *Science*, **295**, 82–91, 2002.
- Larson, R. B., Early star formation and the evolution of the stellar initial mass function in galaxies, *M.N.R.A.S.*, **301**, 569–581, 1998.
- Larson, R. B., Tinsley, B. M., Caldwell, C. N., The evolution of disk galaxies and the origin of S0 galaxies, *Astrophys. J.*, **237**, 692–707, 1980.
- Li, A., Greenberg, J. M., A unified model of interstellar dust, *Astron. Astrophys.*, **323**, 566–584, 1997.
- Lineweaver, C. H., Fenner, Y., Gibson, B. K., The Galactic Habitable Zone

- and the Age Distribution of Complex Life in the Milky Way, *Science*, **303**, 59–62, 2004.
- Lisenfeld, U., Ferrara, A., Dust-to-Gas Ratio and Metal Abundance in Dwarf Galaxies, *Astrophys. J.*, **496**, 145–154, 1998.
- Maiolino, R., Schneider, R., Oliva, E., Bianchi, S., Ferrara, A., Mannucci, F., Pedani, M., Roca Sogorb, M., A supernova origin for dust in a high-redshift quasar, *Nature*, **431**, 533–535, 2004.
- Matsuura, M., Barlow, M. J., Zijlstra, A. A., et al., The global gas and dust budget of the Large Magellanic Cloud: AGB stars and supernovae, and the impact on the ISM evolution, *M.N.R.A.S.*, **396**, 918–934, 2009.
- Mattsson, L., Dust in the early Universe: Evidence for non-stellar dust production or observational errors?, *M.N.R.A.S.*, in press (arXiv:1102.0570)
- McKee, C., Dust Destruction in the Interstellar Medium, in *Interstellar Dust*, Edited by Allamandola, L., Tielens, A. G. G. M., 14 pp, Kluwer Academic Publishers, Dordrecht, 1989.
- Ménard, B., Scranton, R., Fukugita, M., Richards, G., Measuring the galaxy-mass and galaxy-dust correlations through magnification and reddening, *M.N.R.A.S.*, **405**, 1025–1039, 2010.
- Messenger, S., Identification of molecular-cloud material in interplanetary dust particles, *Nature*, **404**, 968–971, 2000.
- Messenger, S., Keller, L. P., Lauretta, D. S., Supernova Olibine from Cometary Dust, *Science*, **309**, 737–741, 2005.
- Michałowski, M. J., Murphy, E. J., Hjorth, J., Watson, D., Gall, C., Dunlop, J. S., Dust grain growth in the interstellar medium of $5 < z < 6.5$ quasars, *Astron. Astrophys.*, **522**, 15, 2010.
- Morgan, H. L., Edmunds, M. G., Dust formation in early galaxies, *M.N.R.A.S.*, **343**, 427–442, 2003.
- Morgan, H. L., Dunne, L., Eales, S. A., Ivison, R. J., Edmunds, M. G., Cold Dust in Kepler's Supernova Remnant, *Astrophys. J.*, **597**, L33–L36, 2003.
- Mouri, H., Taniguchi, Y., Grain Survival in Supernova Remnants and Herbig-Haro Objects, *Astrophys. J.*, **534**, L63–L66, 2000.
- Naab, T., Ostriker, J. P., A simple model for the evolution of disc galaxies: the Milky Way, *M.N.R.A.S.*, **366**, 899–917, 2006.
- Nath, B. B., Laskar, T., Shull, J. M., Dust Sputtering by Reverse Shocks in Supernova Remnants, *Astrophys. J.*, **682**, 1055–1064, 2008.
- Nomoto, K., Tominaga, N., Umeda, H., Kobayashi, C., Maeda, K., Nucleosynthesis yields of core-collapse supernovae and hypernovae, and galactic chemical evolution, *Nuclear Physics A*, **777**, 424–458, 2006.
- Nozawa, T., Kozasa, T., Umeda, H., Maeda, K., Nomoto, K., Dust in the Early Universe: Dust Formation in the Ejecta of Population III Supernovae, *Astrophys. J.*, **598**, 785–803, 2003.
- Nozawa, T., Kozasa, T., Habe, A., Dust Destruction in the High-Velocity Shocks Driven by Supernovae in the Early Universe, *Astrophys. J.*, **648**, 435–451, 2006.
- Nozawa, T., Kozasa, T., Habe, A., Dwek, E., Umeda, H., Tominaga, N., Maeda, K., Nomoto, K., Evolution of Dust in Primordial Supernova Remnants: Can Dust Grains Formed in the Ejecta Survive and Be Injected into the Early Interstellar Medium?, *Astrophys. J.*, **666**, 955–966, 2007.
- Nozawa, T., et al., Formation and Evolution of Dust in Type IIb Supernovae with Application to the Cassiopeia A Supernova Remnant, *Astrophys. J.*, **713**, 356–373, 2010.
- Onaka, T., Kamijo, F., Destruction of interstellar grains by sputtering, *Astrophys. J.*, **64**, 53–60, 1978.
- Pagel, B. E. J., The G-dwarf problem and radio-active cosmochronology, in *Evolutionary phenomena in galaxies*, 23pp., Cambridge University Press, Cambridge and New York, 1989.
- Peacock, J. A., *Cosmological Physics*, pp. 704, Cambridge University Press, Cambridge, 1999.
- Pipino, A., Fan, X. L., Matteucci, F., Calura, F., Silva, L., Granato, G., Maiolino, R., The chemical evolution of elliptical galaxies with stellar and QSO dust production, *Astron. Astrophys.*, **525**, A61, 2011.
- Rho, J., et al., Freshly Formed Dust in the Cassiopeia A Supernova Remnant as Revealed by the Spitzer Space Telescope, *Astrophys. J.*, **673**, 271–282, 2008.
- Rocha-Pinto, H. J., Scalo, J., Maciel, W. J., Flynn, C., Chemical enrichment and star formation in the Milky Way disk. II. Star formation history, *Astron. Astrophys.*, **358**, 869–885, 2000a.
- Rocha-Pinto, H. J., Maciel, W. J., Scalo, J., Flynn, C., Chemical enrichment and star formation in the Milky Way disk. I. Sample description and chromospheric age-metallicity relation, *Astron. Astrophys.*, **358**, 850–868, 2000b.
- Sakon, I., et al., Properties of Newly Formed Dust by SN 2006JC Based on Near- to Mid-Infrared Observation With AKARI, *Astrophys. J.*, **692**, 546–555, 2009.
- Salpeter, E. E., The Luminosity Function and Stellar Evolution, *Astrophys. J.*, **121**, 161–167, 1955.
- Sankrit, R., Williams, B. J., Borkowski, K. J., Gaetz, T. J., Raymond, J. C., Blair, W. P., Ghavamian, P., Long, K. S., Reynolds, S. P., Dust Destruction in a Non-radiative Shock in the Cygnus Loop Supernova Remnant, *Astrophys. J.*, **712**, 1092–1099, 2010.
- Savage, B. D., Sembach, K. R., Interstellar Abundances from Absorption-Line Observations with the Hubble Space Telescope, *Ann. Rev. Astron. Astrophys.*, **34**, 279–330, 1996.
- Schmidt, M., The Rate of Star Formation, *Astrophys. J.*, **129**, 243–258, 1959.
- Schneider, R., Ferrara, A., Salvaterra, R., Omukai, K., Bromm, V., Low-mass relics of early star formation, *Nature*, **422**, 869–871, 2003.
- Schneider, R., Ferrara, A., Salvaterra, R., Dust formation in very massive primordial supernovae, *M.N.R.A.S.*, **351**, 1379–1386, 2004.
- Schneider, R., Omukai, K., Inoue, A. K., Ferrara, A., Fragmentation of star-forming clouds enriched with the first dust, *M.N.R.A.S.*, **369**, 1437–1444, 2006.
- Sibthorpe, B., Ade, P. A. R., Bock, J. J., Chapin, E. L., Devlin, M. J., Dicker, S., Griffin, M., Gundersen, J. O., et al., AKARI and BLAST Observations of the Cassiopeia A Supernova Remnant and Surrounding Interstellar Medium, *Astrophys. J.*, **719**, 1553–1564, 2010.
- Silvia, D. W., Smith, B. D., Shull, J. M., Numerical Simulations of Supernova Dust Destruction. I. Cloud-crushing and Post-processed Grain Sputtering, *Astrophys. J.*, **715**, 1575–1590, 2010.
- Songaila, A., Cowie, L. L., Metal enrichment and Ionization Balance in the Lyman Alpha Forest at $z = 3$, *Astron. J.*, **112**, 335–351, 1996.
- Takeuchi, T. T., Hirashita, H., Testing Intermittence of the Galactic Star Formation History along with the Infall Model, *Astrophys. J.*, **540**, 217–223, 2000.
- Tielens, A. G. G. M., Interstellar Depletions and the Life Cycle of Interstellar Dust, *Astrophys. J.*, **499**, 267–272, 1998.
- Tinsley, B. M., Evolution of the Stars and Gas in Galaxies, *Fundam. Cosmic Phys.*, **5**, 287–388, 1980.
- Todini, P., Ferrara, A., Dust formation in primordial Type II supernovae, *M.N.R.A.S.*, **325**, 726–736, 2001.
- Valiante, R., Schneider, R., Bianchi, S., Andersen, A. C., Stellar sources of dust in the high-redshift Universe, *M.N.R.A.S.*, **397**, 1661–1671, 2009.
- van den Bergh, S., *The Galaxies of the Local Group*, pp. 328, Cambridge University Press, 2000.
- Williams, B. J., Borkowski, K. J., Reynolds, S. P., Blair, W. P., Ghavamian, P., Hendrick, S. P., Long, K. S., Points, S., et al., Dust Destruction in Fast Shocks of Core-Collapse Supernova Remnants in the Large Magellanic Cloud, *Astrophys. J.*, **652**, L33–L36, 2006.
- Yamamoto, T., Hasegawa, H., Grain Formation through Nucleation Process in Astrophysical Environment, *Progress of Theoretical Physics*, **58**, 816–828, 1977.
- Zhukovska, S., Gail, H.-P., Tieloff, M., Evolution of interstellar dust and stardust in the solar neighbourhood, *Astron. Astrophys.*, **479**, 453–480, 2008.

A.K.Inoue (e-mail: akinoue@las.osaka-sandai.ac.jp)